MAX-PLANCK-INSTITUT FÜR PHYSIK UND ASTROPHYSIK
WERNER-HEISENBERG-INSTITUT FÜR PHYSIK

MPI-PAE/Exp.El. 169
December 1986

# A MEASUREMENT OF $\pi^0$-PRODUCTION AT LARGE TRANSVERSE MOMENTUM IN $\pi^-p$, $\pi^+p$ AND pp COLLISIONS AT 300 GeV/c

C. De Marzo, M. De Palma, C. Favuzzi, G. Maggi, E. Nappi,
F. Posa, A. Ranieri, G. Selvaggi and P. Spinelli
Dipartimento di Fisica dell'Universita di Bari
and Istituto Nazionale di Fisica Nucleare, Bari, Italy

A. Bamberger, M. Fuchs, W. Heck, C. Loos, R. Marx, K. Runge,
E. Skodzek, C. Weber, M. Wülker and F. Zetsche
University of Freiburg, Freiburg, Germany

V. Artemiev, Yu. Galaktionov, A. Gordeev, Yu. Gorodkov,
Yu. Kamyshkov, M. Kossov, V. Plyaskin,
V. Pojidaev, V. Shevchenko, E. Shumilov and V. Tchudakov
ITEP, Moscow, U.S.S.R.

J. Bunn*, J. Fent, P. Freund, J. Gebauer, M. Glas, P. Polakos**,
K. Pretzl, T. Schouten***, P. Seyboth,
J. Seyerlein and G. Vesztergombi****
Max-Planck-Institut für Physik und Astrophysik,
München, Germany

NA24-COLLABORATION

submitted to Phys. Rev. D

---

*present adress: CERN, Geneva (Switzerland)

**present adress: Bell Labs Holmdel, New Jersey (U.S.A.)

***present adress: University of Nijmegen (Netherlands)

****on leave of absence from central research Institute for Physics, Budapest (Hungary)

# A MEASUREMENT OF $\pi^0$-PRODUCTION AT LARGE TRANSVERSE MOMENTUM IN $\pi^-$p, $\pi^+$p AND pp COLLISIONS AT 300 GeV/c

C. De Marzo, M. De Palma, C. Favuzzi, G. Maggi, E. Nappi,
F. Posa, A. Ranieri, G. Selvaggi and P. Spinelli
Dipartimento di Fisica dell'Universita di Bari
and Istituto Nazionale di Fisica Nucleare, Bari, Italy

A. Bamberger, M. Fuchs, W. Heck, C. Loos, R. Marx, K. Runge,
E. Skodzek, C. Weber, M. Wülker and F. Zetsche
University of Freiburg, Freiburg, Germany

V. Artemiev, Yu. Galaktionov, A. Gordeev, Yu. Gorodkov,
Yu. Kamyshkov, M. Kossov, V. Plyaskin,
V. Pojidaev, V. Shevchenko, E. Shumilov and V. Tchudakov
ITEP, Moscow, U.S.S.R.

J. Bunn*, J. Fent, P. Freund, J. Gebauer, M. Glas, P. Polakos**,
K. Pretzl, T. Schouten***, P. Seyboth,
J. Seyerlein and G. Vesztergombi****
Max-Planck-Institut für Physik und Astrophysik,
München, Germany

NA24-COLLABORATION

## Abstract

Cross sections for inclusive $\pi^o$-production at large transverse momentum, $p_T$, were measured in $\pi^-$p, $\pi^+$p and pp collisions at 300 GeV/c. The cross section ratio $\frac{\sigma(\pi^- p \to \pi^o X)}{\sigma(\pi^+ p \to \pi^o X)}$ was found to be consistent with unity in the $p_T$ region of 1 to 5 GeV/c. The cross section ratio $\frac{\sigma(\pi^+ p \to \pi^o X)}{\sigma(pp \to \pi^o X)}$ however is growing with increasing $p_T$ and increasing $\pi^o$ c.m.s. rapidity in agreement with parton model expectations, where the partons in the pions have on average higher momenta than in the proton.

---

*present adress: CERN, Geneva (Switzerland)

**present adress: Bell Labs Holmdel, New Jersey (U.S.A.)

***present adress: University of Nijmegen (Netherlands)

****on leave of absence from central research Institute for Physics, Budapest (Hungary)

## 1. Introduction

The study of single particle production at large transverse momentum, $p_T$, in hadron – hadron collisions gave valuable insight into the role of hadronic constituents in hadron – hadron scattering processes. First measurements of inclusive $\pi^o$ production in pp and $\pi$p collisions were reported from the ISR (CERN) [1,2,3] and from Fermilab [4,5]. Large $p_T$ $\pi^o$'s however are mainly fragmentation products of partons and do not directly participate in the parton – parton scattering process. It is therefore difficult to obtain direct information about parton scattering dynamics without the precise knowledge of the fragmentation process.

A more direct way to study parton – parton scattering is the investigation of large $p_T$ direct photons, since the photon couples directly to the quarks. The measurement of direct photon production in $\pi^- p, \pi^+ p$ and pp collisions at 300 GeV/c was the main aim of this experiment, results of which are published in ref. [6].

In this experiment it was essential to detect $\pi^o$'s and $\eta$'s with high efficiency, since unresolved $\pi^o \rightarrow \gamma\gamma$ and $\eta \rightarrow \gamma\gamma$ decays represented the main background to the direct photon detection. For this purpose a large acceptance photon detector with high spatial resolution for electromagnetic showers was employed and operated in an intense particle beam ($\sim 10^7$ particles/sec) of the SPS at CERN. The experimental details and a more extensive description of the data analysis are given in ref. [6].

In this paper we report on $\pi^o$ production cross sections in $\pi^- p$, $\pi^+ p$ and pp collisions at 300 GeV/c. In section 2 of this paper a short description of the apparatus is given. Section 3 contains a discussion of the analysis. In section 4 the experimental results are presented. Section 5 gives the summary.

## 2. Apparatus

A 300 Gev/c momentum beam of negative or positive charge with up to $10^7$ particles/sec impinged on a 1 m liquid $H_2$ target. Protons and pions in the beam were identified using two CEDAR Cerenkov counters. Following the $H_2$ target a set of proportional chambers (22 planes) were used for vertex determination. A fine grained photon position detector (PPD) [7] of 9.6 radiation lengths ($X_o$) thickness was located 8.12 m downstream of the target. Its sensitive area was 3x3 $m^2$ excluding a central hole of 0.5x0.5 $m^2$. It consisted of alternating layers of 1.1 $X_o$ lead sheets and proportional tubes with 0.773 cm wire spacing.

The PPD was followed by a 240 cell ring calorimeter [8] consisting of a 16 $X_o$ lead/scintillator sandwich photon section and a 6 $\lambda_a$ iron/scintillator sandwich hadron section. The acceptance of the calorimeters was between -0.8 and +0.8 in c.m.s. rapidity and $2\pi$ in azimuth. The energy flow through the 56 cm diameter central hole of the ring calorimeter was measured by a downstream calorimeter. An iron wall and a veto counter array positioned upstream of the detector were used to reduce the trigger rate due to upstream interactions and muon background.

The combined PPD/ring calorimeter system was calibrated with electrons and hadrons of 5 GeV to 170 GeV energy. The final calibration was obtained by normalizing the reconstructed $\pi^0$ and $\eta$ masses to the expected values. The systematic uncertainty in the $p_T$ scale was estimated to be $\pm 1$ % and the normalisation uncertainty in the cross section determination to be $\pm 7$ %.

## 3. Analysis

The data were taken at various $p_T$ trigger thresholds to cover the full $p_T$ range accessible. The highest trigger threshold was at $p_T$ >3.75 GeV/c. The trigger events were off-line selected by requiring: i) the reconstructed event vertex to be inside the $H_2$ target fiducial volume, ii) the direction of the triggering shower (as determined from the shower position in the front and the back parts of the fine grained PPD) to point at the $H_2$ target, iii) the total energy measured in all calorimeters to be consistent with the beam energy and iv) the shower signal to be in coincidence with the beam interaction in the hydrogen target (as determined from 30 MHz FLASH ADC's). These cuts removed most of the pile up and muon

backgrounds.

After this event selection the electromagnetic shower with the largest $p_T$ (triggering shower) in an event was paired with every other shower in the event. If a pair of photons was found with an invariant mass between 55 and 210 MeV (470 and 620 MeV) it was assigned to originate from a $\pi^o(\eta)$ decay. The two photon effective mass spectra of these combinations containing the trigger shower are plotted in Fig. 1 for the $\pi^o$-mass region and in Fig. 2 for the $\eta$-mass region. The obtained mass resolutions are $\sigma_{m_{\pi^o}} = 16$ MeV and $\sigma_{m_\eta} = 30$ MeV. In the following $p_T$ refers to the transverse momentum of the $\pi_o$ and the $\eta$ respectively.

The acceptance and the $\pi^o$ reconstruction efficiency were estimated using a Monte Carlo program. This program generated $\pi^o$'s with realistic rapidity and $p_T$ distributions and utilized shower profiles obtained from photon and electron beam calibration runs to simulate the detector response. The Monte Carlo generated events were analysed with the same shower reconstruction program as used with the real data. The Monte Carlo $\gamma\gamma$ mass distributions for $\pi^o$ and $\eta$ events are shown as curves in Fig. 1 and 2 respectively.

The $\pi^0$ decay asymmetry, defined by $A = \frac{|E_1 - E_2|}{E_1 + E_2}$, with $E_1$ and $E_2$ being the energies of the two decay photons, is plotted in Fig. 3. Also shown in Fig. 3 is the asymmetry distribution obtained for the Monte Carlo generated $\pi^o$ events. For the determination of the $\pi^o$-cross section only events with A $\leq$ 0.8 were used.

In order to remove edge effects in the calorimeters the geometrical acceptance was restricted to a c.m.s. rapidity region from -0.65 to +0.52. Finally the measured $\pi^0$ yields were corrected for the effects of the finite energy resolution of the calorimeter. The correction factors were obtained from the Monte Carlo simulation by comparing the number of $\pi^o$'s generated to the number of $\pi^o$'s found by the reconstruction program in the various $p_T$ and rapidity bins.

## 4. Results

In this section we present our measurements of the inclusive $\pi^0$ production cross sections averaged over the c.m.s. rapidity region from -0.65 to +0.52. In Fig. 4 and table I the $\pi^0$ cross sections in $pp$, $\pi^- p$ and $\pi^+ p$ collisions at 300 GeV/c are shown as a function of $p_T$. The errors are of statistical nature only. As mentioned above, there is an additional normalisation uncertainty of $\pm 7$ % and a $p_T$ scale uncertainty of $\pm 1$ %.

Previous results from $pp$ collisions at $\sqrt{s} = 23.5$ GeV in the ISR [1] are shown for comparison in Fig. 4. One can also use inclusive cross sections of $\pi^+$ and $\pi^-$ production in $pp$ and $\pi^- p$ collisions from FNAL [9] at 300 GeV/c to predict inclusive $\pi^0$ cross sections:

$$\sigma(pp \to \pi^0 X) \approx \frac{\sigma(pp \to \pi^+ X) + \sigma(pp \to \pi^- X)}{2} \tag{1}$$

$$\sigma(\pi^- p \to \pi^0 X) \approx \frac{\sigma(\pi^- p \to \pi^+ X) + \sigma(\pi^- p \to \pi^- X)}{2} \tag{2}$$

These predictions are also shown for comparison in Fig. 4. There is good agreement between the various data.

In Fig. 5 the cross section ratios

$$(3) \quad \frac{\sigma(\pi^+ p \to \pi^o X)}{\sigma(pp \to \pi^o X)} \quad \text{and} \quad (4) \quad \frac{\sigma(\pi^- p \to \pi^o X)}{\sigma(\pi^+ p \to \pi^o X)}$$

are plotted versus $p_T$. The ratio (4) is consistent with unity as expected if the detected $\pi^o$'s with large $p_T$ are fragments of quarks or gluons.

The increase of the cross section ratio (3) with increasing $p_T$ has also been observed in a previous experiment [4]. It can be understood in terms of simple parton dynamics where on average the partons in the pion have higher momenta than in the proton. Therefore the available parton parton c.m.s. energy is on average larger in $\pi$p collisions than in pp collisions. This leads to a larger $\pi^o$ production cross section at large $p_T$ in $\pi$p collisions than in pp collisions. At low $p_T$ however

the cross section ratio (3) drops below unity and approaches at $p_T \leq 1$ GeV/c the ratio of the total cross sections $\frac{\sigma_{\pi p}^{tot}}{\sigma_{pp}^{tot}} \sim 0.63$.

The cross section ratio (3) is shown as a function of the c.m.s. $\pi^o$ rapidity in Fig. 6 for $p_T = 5$ GeV/c. The observed rise of this ratio with increasing rapidity can also be understood from the simple parton dynamics discussed above. On average the c.m. system of parton – parton scattering moves along the incident beam direction in the $\pi^+ p$ c.m. system whereas, of course, it is at rest in the $pp$ c.m. system.

## 5. Summary

The inclusive $\pi^o$-production cross sections at large $p_T$ were measured in $\pi^-$p, $\pi^+$p and pp collisions at 300 GeV/c. The cross section ratio $\frac{\sigma(\pi^- p \to \pi^o X)}{\sigma(\pi^+ p \to \pi^o X)}$ was found to be consistent with unity in the $p_T$ range from 1 to 5 GeV/c. The cross section ratio $\frac{\sigma(\pi^+ p \to \pi^o X)}{\sigma(pp \to \pi^o X)}$ is growing with increasing $p_T$ and increasing rapidity. The results are consistent with the expectations from constituent scattering models.

## 6. Acknowledgements

We are grateful for the excellent technical help provided by R. Ferorelli, H. Fessler, W. Fröchtenicht, B. Gordeev, M. Kellner, M. Mongelli, H.J. Osthoff, M. Perchiazzi, H. Röser, A. Sacchetti, J. Seyboth and V. Vinogradov. We wish to thank the staff at CERN for the operation of the SPS accelerator and the H2 beam line and the supporting help of the SPS coordinators.

## REFERENCES


[1] F.W. Büsser et al., Phys. Lett. **46B** (1973) 471

[2] K. Eggert et al., Nucl. Phys. **B98** (1975) 49

[3] For a general review see for instance P. Darriulat, Ann. Rev. of Nucl. and Particle Science **30** (1980) 159

[4] G. Donaldson et al., Phys. Rev. Lett. **36** (1976) 1110

[5] D.C. Carey et al., Phys. Rev. Lett. **33** (1974) 327

[6] C. De Marzo et al., to be published

[7] V. Artemiev et al., NIM **224** (1984) 408

[8] C. De Marzo et al., NIM **217** (1983) 405

[9] H.J. Frisch et al., Phys. Rev. **D27** (1983) 1001 and Phys. Rev. **D19** (1979) 764

**Table 1**

Invariant cross sections for inclusive $\pi^0$ production averaged over the c.m.s. rapidity range from -0.65 to 0.52. The errors are statistical. The systematic uncertainties are $\pm 1\%$ in the $p_T$ scale and $\pm 7\%$ in the normalisation.

| | $E \cdot \frac{d^3\sigma}{dp^3}(cm^2 \cdot GeV^{-2} \cdot c^3)$ | | |
|---|---|---|---|
| $p_T$ $(Gev/c)$ | $pp \to \pi^0 + X$ | $\pi^+ p \to \pi^0 + X$ | $\pi^- p \to \pi^0 + X$ |
| 1.25 | $(1.23 \pm 0.06) \cdot 10^{-28}$ | $(8.36 \pm 0.70) \cdot 10^{-29}$ | $(8.28 \pm 0.39) \cdot 10^{-29}$ |
| 1.75 | $(1.10 \pm 0.15) \cdot 10^{-29}$ | $(7.16 \pm 1.80) \cdot 10^{-30}$ | $(7.26 \pm 0.88) \cdot 10^{-30}$ |
| 2.25 | $(1.07 \pm 0.08) \cdot 10^{-30}$ | $(1.06 \pm 0.11) \cdot 10^{-30}$ | $(9.50 \pm 0.50) \cdot 10^{-31}$ |
| 2.75 | $(1.50 \pm 0.30) \cdot 10^{-31}$ | $(1.68 \pm 0.38) \cdot 10^{-31}$ | $(1.32 \pm 0.17) \cdot 10^{-31}$ |
| 3.25 | $(1.61 \pm 0.03) \cdot 10^{-32}$ | $(1.74 \pm 0.04) \cdot 10^{-32}$ | $(1.88 \pm 0.02) \cdot 10^{-32}$ |
| 3.75 | $(3.05 \pm 0.13) \cdot 10^{-33}$ | $(4.18 \pm 0.22) \cdot 10^{-33}$ | $(3.87 \pm 0.09) \cdot 10^{-33}$ |
| 4.25 | $(4.70 \pm 0.12) \cdot 10^{-34}$ | $(7.81 \pm 0.25) \cdot 10^{-34}$ | $(7.94 \pm 0.09) \cdot 10^{-34}$ |
| 5.00 | $(5.35 \pm 0.26) \cdot 10^{-35}$ | $(1.23 \pm 0.06) \cdot 10^{-34}$ | $(1.10 \pm 0.02) \cdot 10^{-34}$ |
| 6.00 | $(4.41 \pm 0.87) \cdot 10^{-36}$ | $(6.95 \pm 1.70) \cdot 10^{-36}$ | $(9.27 \pm 0.64) \cdot 10^{-36}$ |
| 7.00 | | $(1.33 \pm 0.96) \cdot 10^{-36}$ | $(7.79 \pm 2.30) \cdot 10^{-37}$ |

## FIGURE CAPTIONS

1. Two photon invariant mass spectrum in the $\pi^o$ mass region with $4< p_T <5$ GeV/c. The distribution has a $\sigma$ of 16 MeV. The solid curve gives the result of a Monte Carlo simulation. (Due to the cuts in the reconstruction procedure the mass values come out somewhat lower than the true values.)

2. Two photon invariant mass spectrum in the $\eta$ region with $3< p_T <4$ GeV/c. The $\eta$ mass peak has a $\sigma$ of 30 MeV. The solid curve gives the result of the Monte Carlo calculation, the dashed line is an estimate of the combinatorial background. (Due to the cuts in the reconstruction procedure the mass values come out somewhat lower than the true values.)

3. Asymmetry distribution $A = \frac{|E_1-E_2|}{E_1+E_2}$ of reconstructed $\pi^o$ decays with $4< p_T <5$ GeV/c. The solid curve represents the result of the Monte Carlo simulation.

4. Invariant cross sections for inclusive $\pi^o$ production in pp, $\pi^-$p and $\pi^+$p collisions at 300 GeV/c. The data are compared to results from pp collisions in the ISR [1] and from pp and $\pi^-$p collisions at FNAL [9](see text).

5. Cross section ratios of inclusive $\pi^o$ production for different incident beam particles versus $p_T$ and $x_T$, with $x_T = \frac{2p_T}{\sqrt{s}}$.

6. Cross section ratio of inclusive $\pi^o$ production in $\pi^+$p and pp collisions as a function of the c.m.s. $\pi^o$ rapidity.

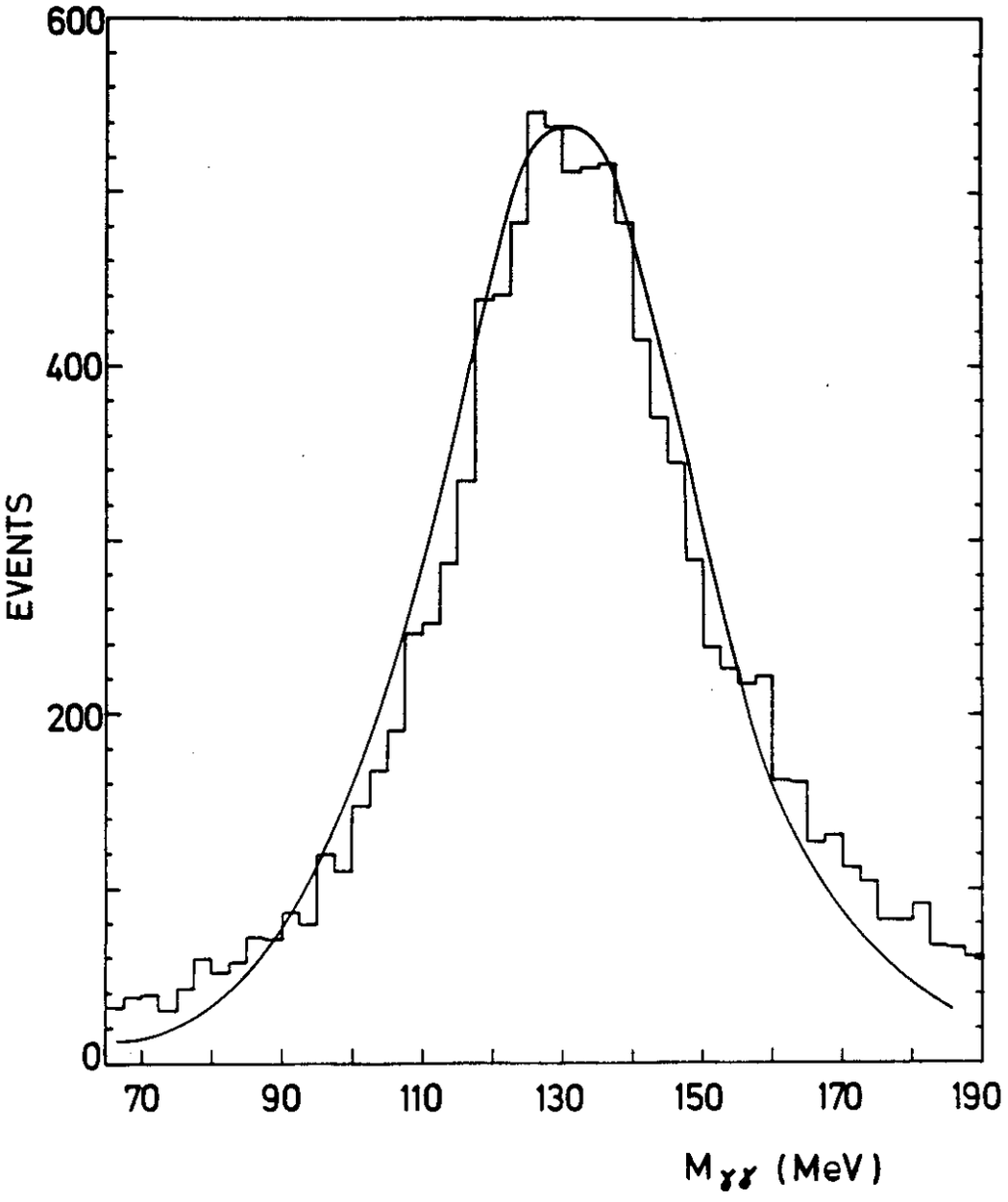


Fig. 1

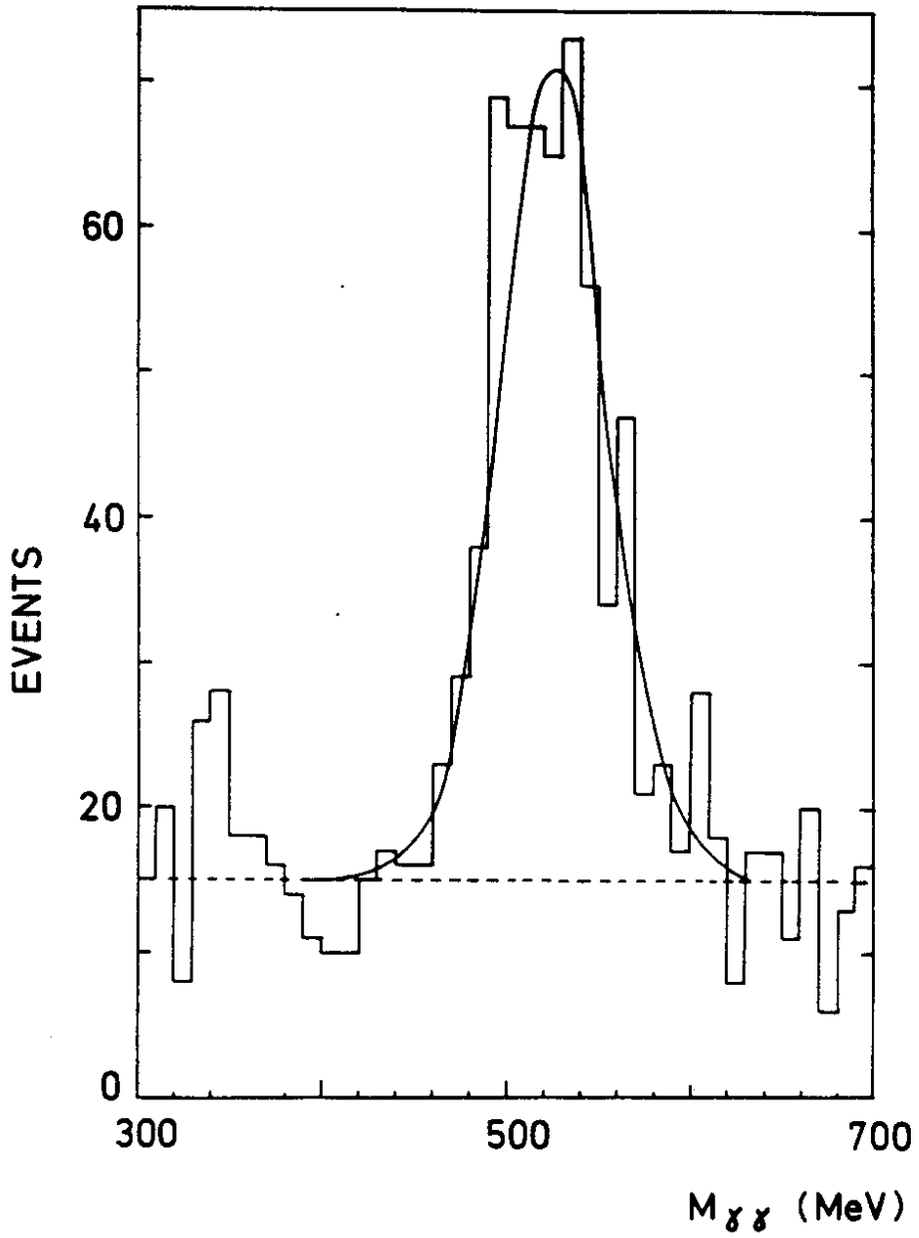


Fig. 2

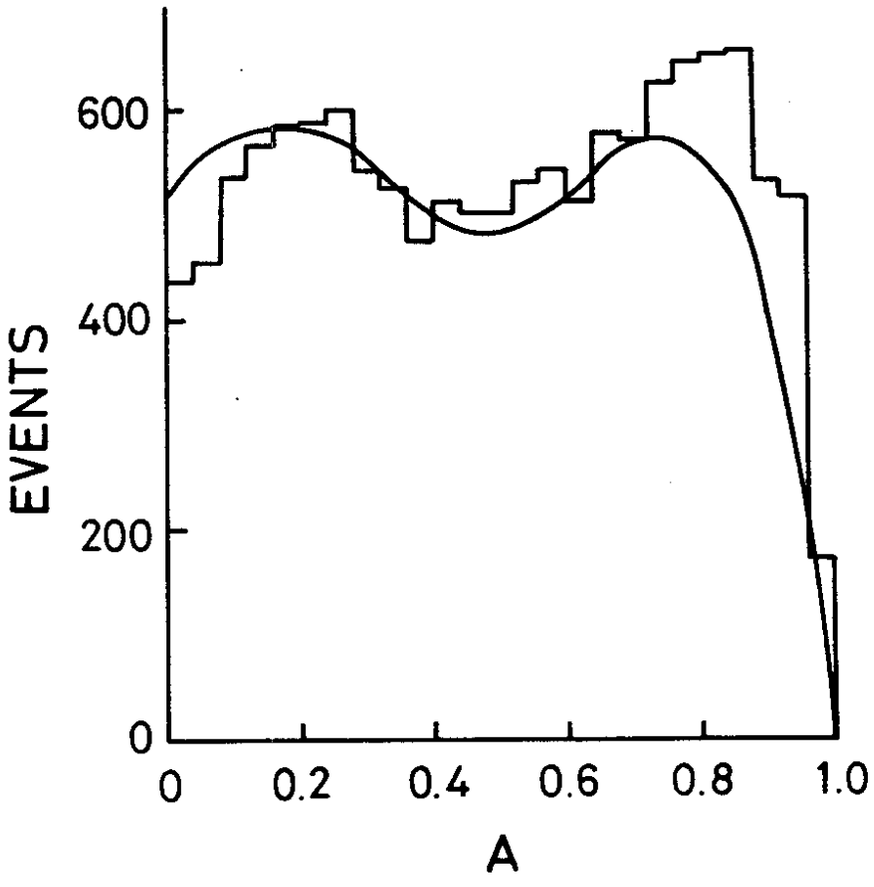


Fig. 3

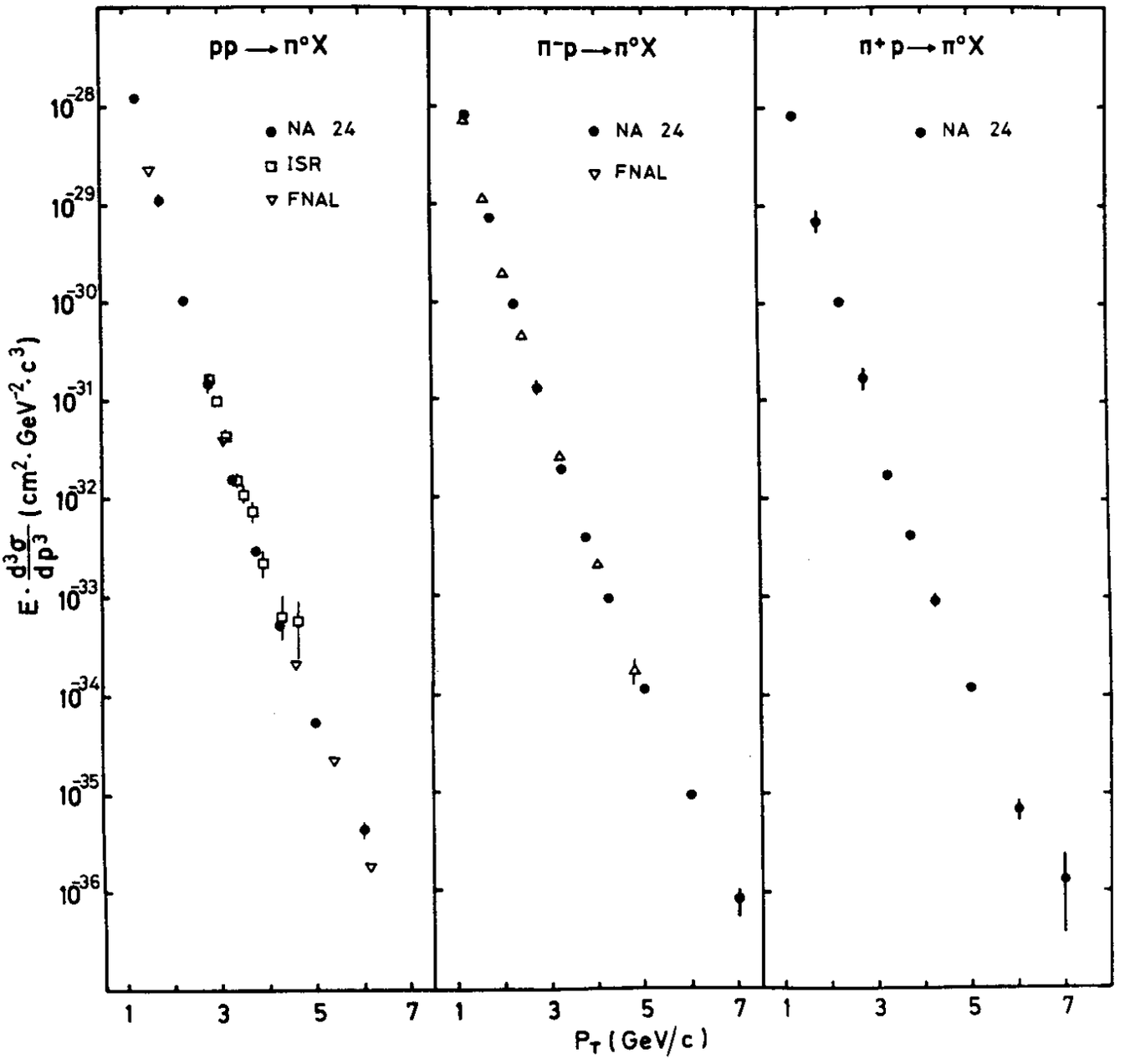
pp → π°X
π⁻p → π°X
π⁺p → π°X
NA 24
ISR
FNAL
$E \cdot \frac{d^3\sigma}{dp^3}$ (cm$^2$. GeV$^{-2}$. c$^3$)
$P_T$ (GeV/c)

Fig. 4

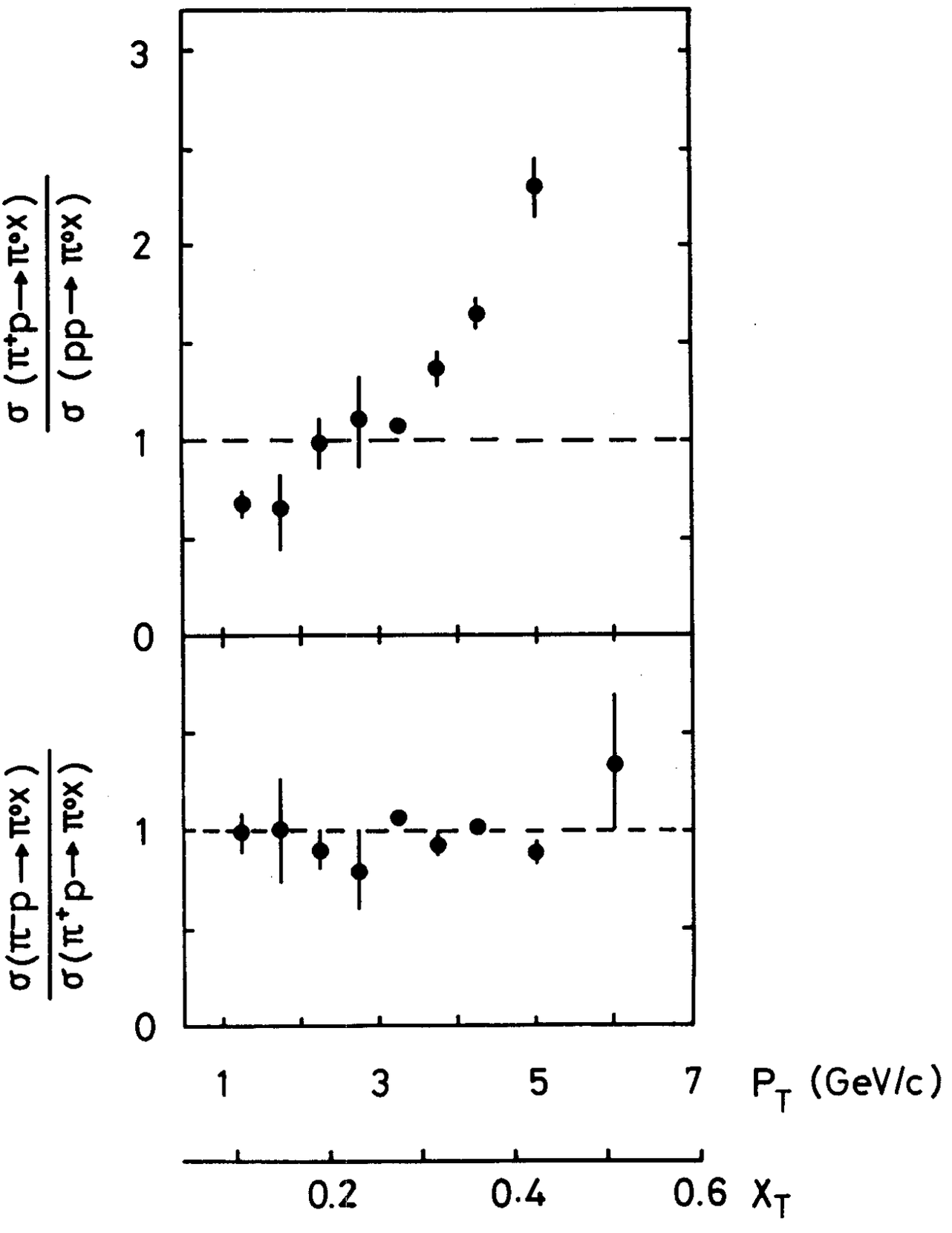
$\frac{\sigma(\pi^+ p \to \pi^0 X)}{\sigma(pp \to \pi^0 X)}$
$\frac{\sigma(\pi^- p \to \pi^0 X)}{\sigma(\pi^+ p \to \pi^0 X)}$
3
2
1
0
1
0
1
3
5
7
$P_T$ (GeV/c)
0.2
0.4
0.6
$X_T$

Fig. 5

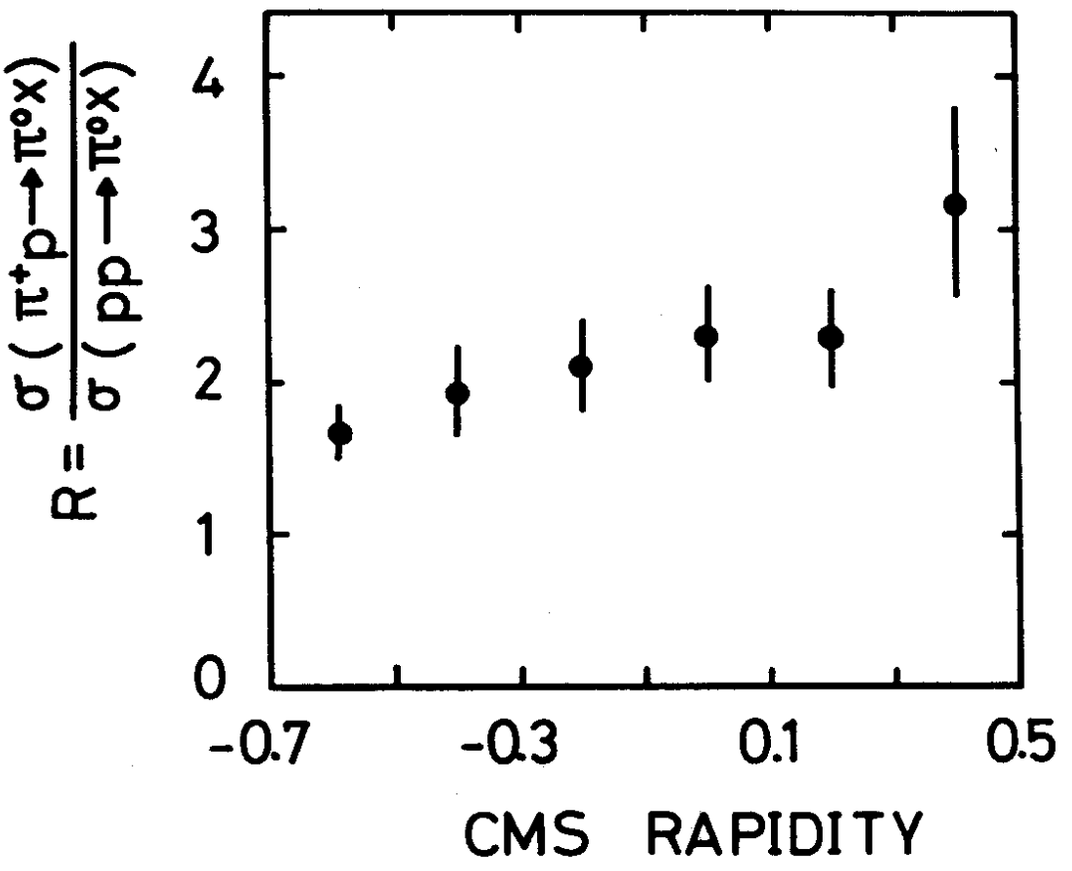
$R = \frac{\sigma(\pi^+ p \to \pi^0 X)}{\sigma(pp \to \pi^0 X)}$
4
3
2
1
0
-0.7
-0.3
0.1
0.5
CMS RAPIDITY

Fig. 6

Druck: Dokumentation Astrophysik Karl-Schwarzschild-Str. 1 · 8046 Garching bei München